


Synthesis and characterization of poly(ester amide amide)s of different alkylene chain lengths

Clément Girard¹ · Manisha Gupta² · Abdelaziz Lallam¹ · Denis V. Anokhin^{3,4} · Polina V. Bovsunovskaya^{3,5} · Azaliya F. Akhyamova^{3,5} · Alexey P. Melnikov^{3,5} · Alexey A. Piryazev^{3,5} · Alexander I. Rodygin^{3,5} · Andrey A. Rychkov^{3,5} · Kseniia N. Grafskaya³ · Ekaterina D. Shabratova³ · Xiaomin Zhu² · Martin Möller² · Dimitri A. Ivanov^{3,6} 

Received: 27 December 2017 / Revised: 17 April 2018 / Accepted: 7 May 2018 /
Published online: 7 June 2018
© Springer-Verlag GmbH Germany, part of Springer Nature 2018

Abstract In this work, a series of aliphatic biodegradable poly(ester amide amide) polymers was synthesized by melt polycondensation of a tailor-made amide-containing monomer based on 1,4-diaminobutane and ϵ -caprolactone and different dicarboxylic acid methyl esters with even number of methylene groups. The synthesized polymers were characterized by ¹H NMR, FT-IR spectroscopy, GPC, SAXS and

Clément Girard and Manisha Gupta have contributed equally to the work.

Manisha Gupta: Deceased 1st November 2017.

✉ Xiaomin Zhu
zhu@dw1.rwth-aachen.de

✉ Dimitri A. Ivanov
dimitri.ivanov@uha.fr

¹ Laboratoire de Physique et Mécanique Textile, Université de Haute Alsace, 68093 Mulhouse, France

² DWI – Leibniz-Institute for Interactive Materials e.V. and Institute for Technical and Macromolecular Chemistry, RWTH Aachen University, Forckenbeckstraße 50, 52056 Aachen, Germany

³ Moscow Institute of Physics and Technology (State University), Institutskiy per. 9, Dolgoprudny, Russia 141700

⁴ Institute for Problems of Chemical Physics RAS, Semenov Av. 1, Chernogolovka, Moscow Region, Russia 142432

⁵ Faculty of Fundamental Physical and Chemical Engineering, Lomonosov Moscow State University, GSP-1, 1-51 Leninskie Gory, Moscow, Russia 119991

⁶ Institut de Sciences des Matériaux de Mulhouse (CNRS UMR 7361), 15 rue Jean Starcky, B.P 2488, 68057 Mulhouse, France

WAXS. DSC results show that the melting point is located at about 150 °C for all polymers. X-ray scattering experiments in small and wide angles reveal formation of crystals with extended-chain conformation resulting in strict periodicity of electron density along the main chain. TGA data indicate the high thermal stability of polymers to temperatures above 350 °C, which are much above the melting point. The obtained characteristics of the newly synthesized PEAs can open new perspectives for melt processing to fabricate films, highly oriented fibers and injection-molded parts with good thermal stability and mechanical performance.

Keywords Poly(ester amide amide)s · Biodegradable polymers · Melt polycondensation · Small-angle X-ray scattering · Wide-angle X-ray scattering

Introduction

Biodegradable polymers have emerged as a solution for the global environmental pollution problem caused by the non-degradable waste products [1, 2]. Nowadays, they are increasingly used in different fields ranging from packaging to biomedical applications. Aliphatic polyesters such as poly(lactic acid), poly(glycolic acid) and their copolymers are typical examples of synthetic biodegradable polymers. However, they still have limited applications due to poor mechanical properties and insufficient processibility. On the other hand, aliphatic polyamides have good mechanical and thermal stability but are non-biodegradable. The desired combination of properties can be achieved by synthesis of poly(ester amide)s (PEAs) with either randomly distributed amide groups [3–14] or with well-defined amide blocks in the polymer chain [15–21]. The poly(ester amide)/polyamide copolymers of different microstructures, i.e., random, alternating or segmented, can be prepared depending on the monomer nature and synthetic route.

Segmented PEAs containing both rigid amide and flexible ester blocks exhibit a microphase-separated structure typical of thermoplastic elastomers [22–28]. Such polymers form homogeneous melts upon heating above the melting temperature of hard segments and thus can be easily melt processed. During cooling, the microphase separation of the rigid amide and soft ester domains takes place. The crystalline lamellae of the rigid phase serve as a thermoreversible physical network within the elastic ester phase. Therefore, the properties of PEAs can be tuned in a wide range by varying the amide and ester contents [22, 23, 29].

Several groups have synthesized aliphatic segmented PEAs having uniform amide blocks. Preformed bisamide-diols, oligoesters and bisamide-esters were copolymerized with diols and dimethyl adipates to obtain high molecular weight segmented PEAs [18–21, 30]. The effect of hard-to-soft segments' ratio on the physical–chemical properties of PEAs was studied in detail. Thus, Lips and colleagues [22] synthesized high molecular weight segmented PEAs by melt polycondensation of preformed bisamide-diol based on 1,4-diaminobutane and ϵ -caprolactone with 1,4-butanediol and dimethyl adipate. The increase in hard segment content from 10 to 85 mol% results in enhancement of the mechanical modulus from 70 to 524 MPa

and the stress at break from 8 to 28 MPa. For all the synthesized polymers, a single glass transition was observed, which increases with the increase in hard segment content indicating the presence of a homogeneous amorphous phase. In addition, two endothermic peaks at low and high temperatures were attributed to melting of the crystals formed by single ester amide (EA) sequences and by two or more EA sequences, respectively. The low-temperature transition was independent from polymer composition, while the high-temperature transition peak was found to move to higher temperatures with the increase in the hard segment content.

Garg and co-authors [23] have synthesized segmented PEAs consisting of single amide groups, two adjacent amide groups or three adjacent amide groups by melt polycondensation of amide-containing monomers, butylene adipate and 1,4-butanediol, and the preformed monomers were α,ω -diol, α,ω -aminoalcohol and α,ω -diamine with an in-built amide group, respectively. Varying amount of these preformed monomers in the feed leads to different contents of amide groups in the PEAs and thus result in different physical–chemical properties of the synthesized PEAs. Among all these materials the copolymers containing two adjacent amide groups exhibited an interesting crystalline structure, which is formed by both ester and amide groups. In this work, we focus on the homopolymers from α,ω -amino alcohols and dicarboxylic acid methyl esters, which are two monomers for the synthesis of polymers with two adjacent amide groups, and address their crystalline structures and physical–chemical properties. In these polymers, the molar ratio of ester to amide groups is 1:2, so they are called poly(ester amide amide)s (PEEAs), and the number of adjacent amide groups can be 2 and 4. In principle, a microphase-separated structure cannot be expected for PEEAs; however, the presence of ester groups should impart the biodegradability.

Materials

ϵ -Caprolactone (97%), 1,4-diaminobutane (99%) and dimethyl adipate (DMA) (98%) were purchased from Aldrich. Dimethyl suberate (DMSUB) (99%) and dimethyl sebacate (DMSEB) (97%) were obtained from Alfa Aesar. Titanium IV isopropoxide was purchased from ABCR. 2-Propanol (absolute) was purchased from Fluka, and 2,2,2-trifluoroethanol was purchased from Sigma-Aldrich. The solvents such as tetrahydrofuran (THF), dimethylformamide (DMF) and methanol were purchased from VWR. All the chemicals were used without additional purification.

Synthesis

Synthesis of monomer

Tailor-made monomer α,ω -aminoalcohol ($\text{HO}(\text{CH}_2)_5\text{CONH}(\text{CH}_2)_4\text{NH}_2$, AA) was prepared according to the procedure described in the literature [31]. A solution of ϵ -caprolactone (100.0 g, 0.88 mol) in THF (80 mL) was dropped to a solution of 1,4-diaminobutane (271.04 g, 3.08 mol) in THF (260 mL). This reaction mixture

was stirred for 20 h at room temperature. Afterward, the excess of 1,4-diaminobutane and THF was removed in high vacuum (10^{-2} mbar) by slow heating to 60 °C. The product was then dissolved in methanol and precipitated in cold diethyl ether. The white product was filtered and dried in vacuum with 80% yield (mp 75 °C).

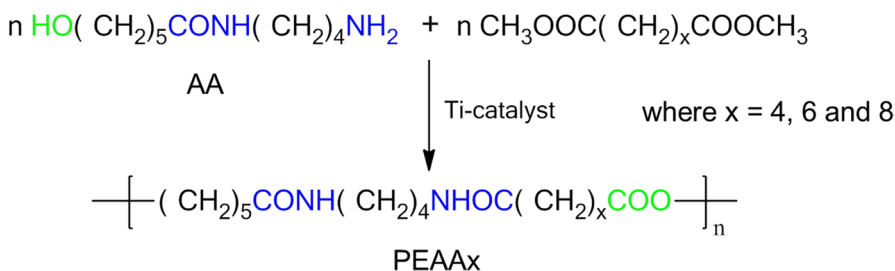
Synthesis of poly(ester amide amide)s

The PEAAx were synthesized by a two-step melt polycondensation according to Scheme 1. Equimolar ratio of tailor-made monomer AA and dicarboxylic esters of different alkylene chain length (e.g., dimethyl adipate, dimethyl sebacate and dimethyl sebacate) were added to a glass reactor, which was equipped with a mechanical stirrer. Ti(IV) isopropoxide (5 mg/g of dicarboxylic acid ester) in isopropanol (1% w/w) was then added to the reactor under inert atmosphere. The reaction mixture was then slowly heated to 170 °C under a pressure of 100 mbar. Under stirring, the heating was continued for another 5 h. Further reaction was performed by heating the reaction mixture slowly to 180 °C and by decreasing the pressure to 1 mbar. At the final temperature, the reaction was carried out for 4 h in a high vacuum of 10^{-2} mbar. At the end, the resulting melt was retrieved from the reactor, dissolved in 2,2,2-trifluoroethanol and precipitated in diethyl ether. The procedure was repeated three times. The final product dried at 50 °C in a vacuum oven for 8 h. The synthesized polymers were found to be soluble in conventional solvents for polyamides such as formic acid, trifluoroacetic acid, trifluoroethanol and phenol, whereas they are not soluble in DMF and THF.

Characterization techniques

Nuclear magnetic resonance (NMR) spectroscopy

^1H NMR spectra were obtained on a Bruker DPX 300 operating at 300 MHz. Deuterated trifluoroacetic acid (D-TFA) was used as solvent with TMS as internal standard.



Scheme 1 Synthesis of PEAAx by melt polycondensation

Elemental analysis

Chemical composition of synthesized PEAA was evaluated by elementary analysis of carbon, hydrogen and nitrogen using Carlo Erba MOD 1106 instrument.

Fourier transform infrared spectroscopy (FT-IR)

FT-IR spectra were collected using Thermo Nicolet Model Nexus 470 spectrophotometer equipped with a DTGS detector from 100 signal-averaged scans with 8 cm^{-1} resolution. The samples were in the form of a thin polymer film of ca. $25\text{ mm} \times 10\text{ mm}$ placed on KBr disk. The data were collected in the range of $500\text{--}4000\text{ cm}^{-1}$.

Gel permeation chromatography (GPC)

GPC measurements were taken on a Waters 1515 Isocratic HPLC pump, a Viscotek 250 model refractive index detector, a Waters 2707 auto-sampler, a PSS PFG guard column followed by 2 PFG-linear-XL ($7\text{ }\mu\text{m}$, $8 \times 300\text{ mm}$) columns in series at $40\text{ }^\circ\text{C}$. Hexafluoroisopropanol (HFIP, Biosolve) with potassium trifluoroacetate (3 g/L) and toluene (2.5 mL/L) was used as eluent at a flow rate of 0.8 mL/min . The molecular weights were calibrated with PMMA standards (Polymer Laboratories, $M_p = 580\text{ Da}$ up to $M_p = 7.1 \times 10^6\text{ Da}$).

Thermogravimetric analysis

A TG-209 (Netzsch) instrument was used to study the thermal stability of the synthesized polymers. To this purpose, $2\text{--}4\text{ mg}$ of the sample was placed in a standard Netzsch aluminum pan and heated in nitrogen from 30 to $700\text{ }^\circ\text{C}$ at a heating rate of $10\text{ }^\circ\text{C/min}$.

Differential scanning calorimetry

DSC measurements were taken on a DSC-204 (Netzsch, Germany). For the experiments, $5\text{--}8\text{ mg}$ of sample was sealed in a standard Netzsch aluminum pan and was heated from 0 to $220\text{ }^\circ\text{C}$ at a heating rate of $10\text{ }^\circ\text{C/min}$. The flow rate of nitrogen was $10\text{ cm}^3/\text{min}$. The temperature of the phase transition was determined as the onset of the corresponding peak on the DSC curve.

SAXS/WAXS

Small- (SAXS) and wide-angle (WAXS) X-ray scattering data were measured on a XeuSS diffractometer (Xenocs) equipped with a GeniX3D ($\lambda = 1.54\text{ \AA}$) source providing a beam of ca. $300 \times 300\text{ }\mu\text{m}^2$ in size. Two-dimensional SAXS patterns were recorded with a Pilatus 300 k detector at the sample-to-detector distance of 1324.44 mm . Two-dimensional WAXS images were collected with a Rayonix LX170-HS detector positioned 91 mm away from the sample. The modulus of the

scattering vector s ($|s|=2\sin\Theta/\lambda$, where Θ is the Bragg angle and λ -the wavelength) was calibrated using seven diffraction orders of silver behenate.

Results and discussions

In this work, the polycondensation of α,ω -aminoalcohol AA with dicarboxylic acid methyl esters of different alkylene chain length (cf. Scheme 1) results in PEAAx with a theoretical ratio of ester to amide groups 1:2. The synthesized polymers are denoted as PEAA4, PEAA6 and PEAA8, where the digit indicates the number of the methylene groups in the dicarboxylic acid methyl ester.

^1H NMR spectroscopy was used to determine the chemical composition of PEAA4, PEAA6 and PEAA8. The ratio of ester to amide groups in PEAAx ($X_{e/a}$) was calculated from ^1H NMR spectra according to Eq. (1):

$$X_{e/a} = I_e/I_a \quad (1)$$

where I_e and I_a stand for the integral intensities of protons at $\delta=4.1$ ppm and $\delta=3.4$ ppm, which correspond to CH_2 groups connected directly to oxygen and nitrogen atom, respectively. An example of a ^1H NMR spectrum of PEAAx is presented in Fig. 1. The experimental values of $X_{e/a}$ in the PEEAs summarized in Table 1 are in good agreement with the theoretical values. A small deviation from the theoretical composition can be accounted for by loss of a small amount of

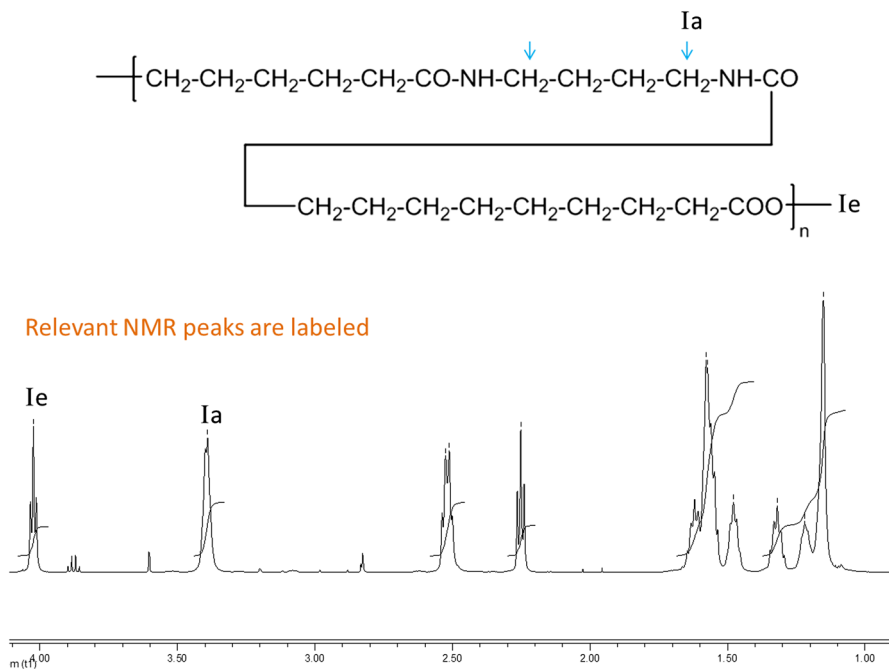


Fig. 1 ^1H NMR spectrum of PEAA8 in D-TFA

Table 1 Chemical composition of PEAAAs

Polymer	Monomer 1, g	Monomer 2, g	$X_{e/a}$	Elemental composition					
				Theoretical			Experimental		
				C, %	H, %	N, %	C, %	H, %	N, %
PEAA4	AA, 10	DMA, 8.71	1:1.84	61.54	8.97	8.97	61.03	8.85	8.60
PEAA6	AA, 10	DMSUB, 10.11	1:1.88	63.53	9.41	8.23	62.82	11.68	7.99
PEAA8	AA, 10	DMSEB, 11.52	1:1.84	65.22	9.78	7.61	64.52	9.78	7.22

dicarboxylic methyl esters during the precondensation step. The chemical composition was also confirmed by elemental analysis. The experimental contents of different elements coincide well with the theoretical ones (cf. Table 1). According to GPC data, all synthesized polymers exhibit a monomodal molecular weight distribution and relatively high molecular weight (cf. Table 2). The polydispersity index (PDI) is about 2, which is typical for polymers prepared via polycondensation. It is noteworthy that the synthetic route used in the present work may result in the formation of both EAAEAA and EAAAAE sequences. Their ratio should theoretically be 1:1 and unfortunately cannot be measured by NMR spectroscopy. The presence of both sequences in the polymer chain is most probably responsible for the low crystallinity and broad distribution of crystalline domain size as indicated by broad melting peaks.

The FT-IR spectra of the synthesized polymers taken for the wavenumber regions of 3600–2700 and 1800–650 cm^{-1} are presented in Figs. 1b and 2a, respectively. All PEAAAs show the characteristic IR peaks at ~ 1732 (ν CO ester), ~ 1635 cm^{-1} (amide I, (ν CO) and ~ 1541 cm^{-1} (amide II ν CN + CO ν NH bend), which reveal the presence of both ester and amide bonds in the polymer backbone. The IR spectra of the PEAAAs also indicate the appearance of a strong H-bond peak at ~ 3300 cm^{-1} (ν NH H-bonded) with a shoulder at ~ 3400 cm^{-1} (ν OH H-bonded). Several weaker bands at 1474 cm^{-1} (NH vicinal CH_2 bend), ~ 1420 cm^{-1} (CO vicinal CH_2 bend), ~ 1260 cm^{-1} (amide III), ~ 693 cm^{-1} (amide V) and ~ 585 cm^{-1} (amide VI) show the crystallization of amide rigid blocks [32]. In nylon 6, the most stable crystalline polymorphs are α and γ phases. The main peaks of the synthesized PEAAAs and the characteristic peaks of nylon 6 in α and γ crystal phases are listed in Table 3. A more detailed analysis of the IR bands shows that the crystal structure of PEAA4 is a mixture of α and γ modifications of nylon 6, whereas in PEAA6 and PEAA8, only α crystalline phase was observed.

Table 2 Molecular weight and polydispersity of PEAAAs

Polymer	M_n (kDa)	M_w (kDa)	PDI
PEAA4	15.7	35.5	2.26
PEAA6	34.9	50.7	1.45
PEAA8	20.5	55.5	2.70

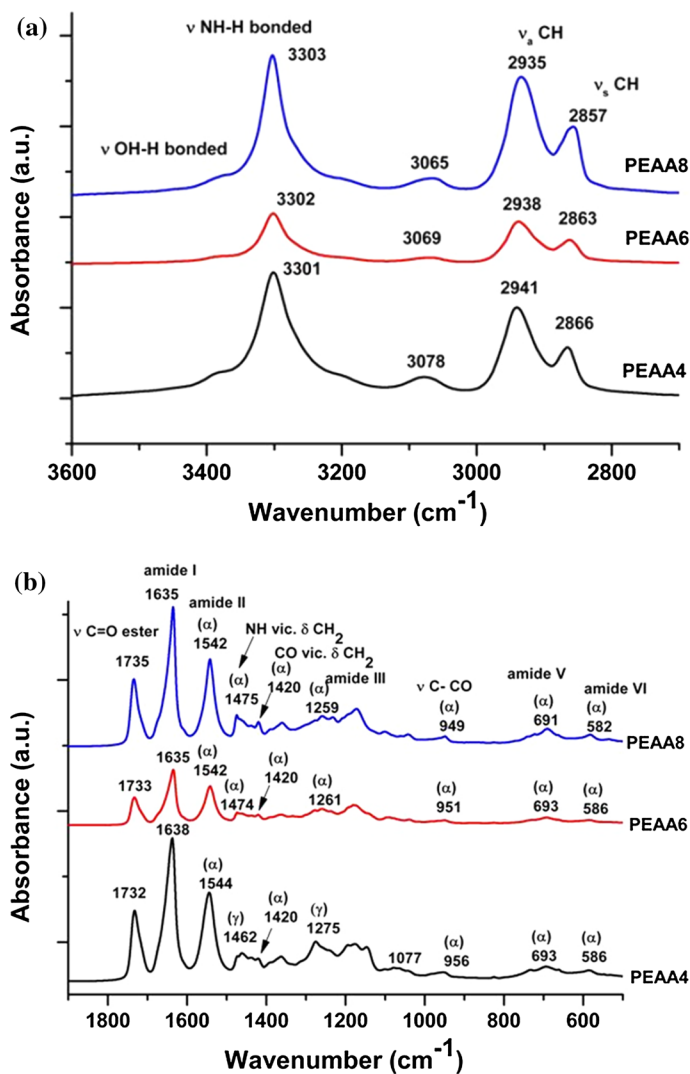


Fig. 2 FT-IR spectra of the PEEA series for the wave number region **a** 3600–1800 cm⁻¹ and **b** 1800–600 cm⁻¹ measured at room temperature

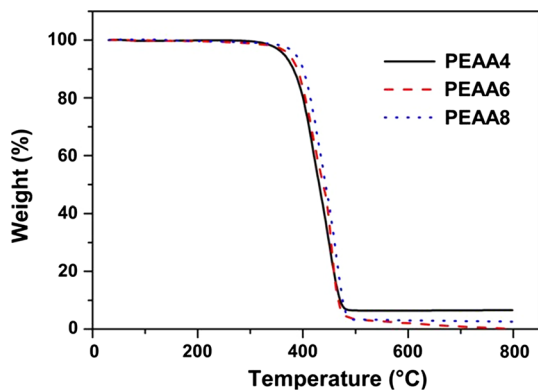
The thermal stability of PEEAs was investigated with the help of TGA under nitrogen atmosphere. As shown in Table 4, the PEEAs are stable up to 350 °C. The TGA curves reveal similar single-stage degradation for all studied polymers (cf. Fig. 3). The high thermal stability allows processing them in the melt. The thermal behavior of the synthesized PEEAs was analyzed by the DSC technique. To this end, the thermal history of the samples was erased during the first heating. The DSC traces corresponding to the cooling and the second heating are presented in Fig. 4. It can be seen that the glass transition temperatures (T_g) slightly decrease with the

Table 3 Assignment of FT-IR characteristic peaks in the synthesized PEAA4s and their comparison with the ones of nylon 6

Assignment ^a	Nylon6 (α)	Nylon6 (γ)	PEAA4	PEAA6	PEAA8
ν NH H-bonded			3301	3302	3303
ν_a			2941	2938	2935
ν_s			2866	2863	2857
Amide I			1638	1635	1635
Amide II	~ 1540	~ 1560	1544 (α)	1542 (α)	1542 (α)
NH vic. CH ₂ bend	~ 1475			1474 (α)	1475 (α)
CH ₂ bend	1464	1463	1462 (γ)		
CO vic. CH ₂ bend	1417		1420 (α)	1420 (α)	1420 (α)
Amide III	1265	1269	1275 (γ)	1261 (α)	1259 (α)
ν C–CO	959	977	956 (α)	951 (α)	949 (α)
Amide V	691	712	693 (α)	693 (α)	691 (α)
Amide VI	579	623	586 (α)	586 (α)ho	582 (α)

^a ν stretching mode**Table 4** Thermal properties of the synthesized PEAA4s

Polymer	T_d^a (°C)	T_g^b (°C)	T_{m1}^b (°C)	T_{m2}^b (°C)	ΔH_m^b (J/g)	T_c^b (°C)	ΔH_c^b (J/g)
PEAA4	385	13.4	150.6	159.3	24.7	133.4	22.5
PEAA6	412	9.9	145.3	160.0	34.6	133.8	29.7
PEAA8	405	8.4	145.8	154.0	38.0	127.9	30.4

^aOnset of decomposition as measured by TGA^bMaximum of the peak measured by DSC**Fig. 3** TGA thermograms of the studied polymers

increase in the alkylene spacer length, which reflects the increasing flexibility of the backbone. The crystallization temperature (T_c) of PEAA4 and PEAA6 is 133.4 and 133.8 °C, respectively (cf. Fig. 4a, Table 4). Although their T_c is similar, the

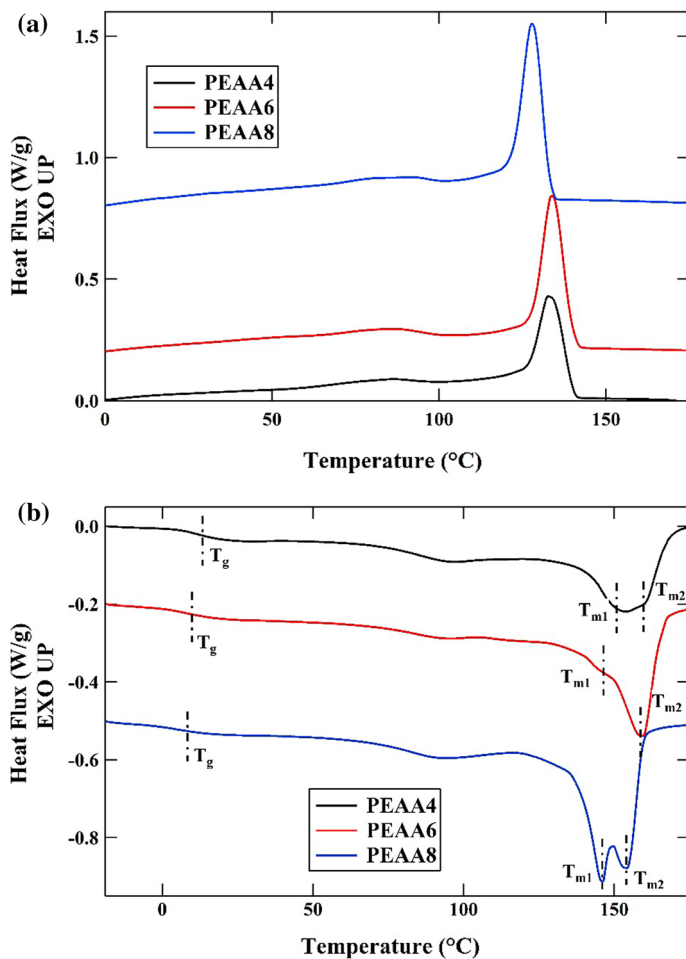


Fig. 4 DSC of PEAA4, PEAA6 and PEAA8: **a** cooling scan and **b** second heating scan (performed at a heating and cooling rate of 10 K/min)

enthalpy of crystallization (ΔH_c) for the latter sample is much higher. For PEAA8, a further increase in ΔH_c and decrease in T_c was detected (Table 4). It is reasonable to assume that crystallinity of the samples enhances with the increase in the alkylene chain length of the dicarboxylic esters because of increased chain flexibility. The second heating curves show a single melting peak for all samples with close melting temperature values T_m in the range of 134–137 °C (cf. Fig. 4b). On the other hand, in line with the previously mentioned values of ΔH_c , the enthalpy of melting (ΔH_m) significantly increases from PEAA4 to PEAA8. This observation further confirms that the longer flexible alkylene spacer results in formation of better quality crystals.

It is noteworthy that the polymers exhibit complex thermal behavior typical of the family of semirigid-chain semicrystalline polymers such as PEEK, PET, PTT and others. In particular, they reveal the presence of multiple melting, which is

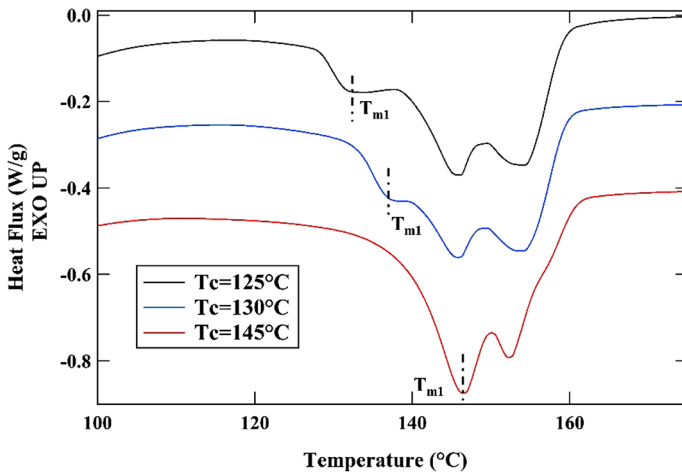


Fig. 5 DSC heating traces of PEAA8 after isothermal melt crystallization at the indicated temperatures

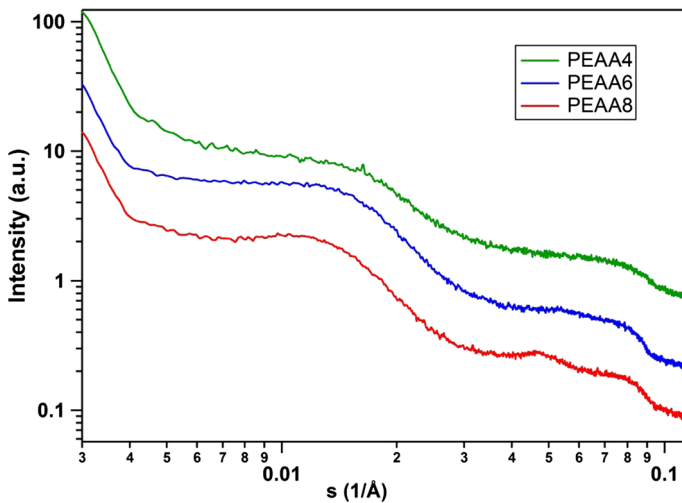


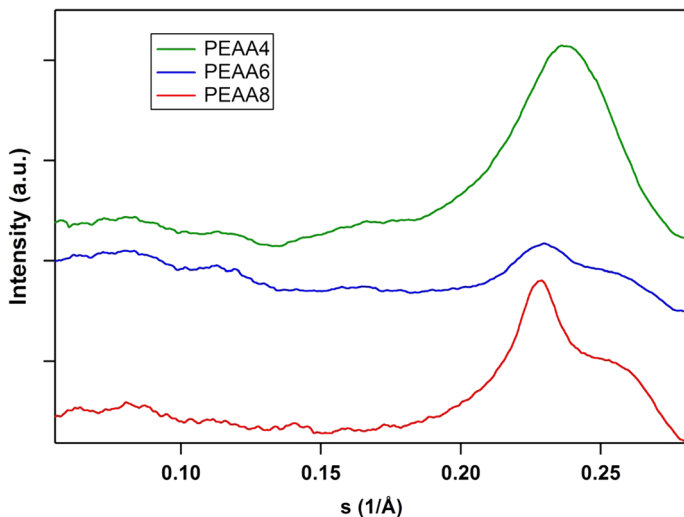
Fig. 6 SAXS curves of PEEA samples measured at room temperature

sometimes assigned to crystal reorganization occurring on heating. In order to investigate this in more detail, we have melt-crystallized the polymers isothermally from the melt. The obtained results are exemplified for the case of the PEAA8 sample in Fig. 5. It can be seen that the low melting peak is located at temperatures about 10–15 °C above the previous isothermal crystallization, which is typical observation for this class of polymers [33, 34]. A detailed analysis of the semicrystalline structure was performed by X-ray scattering technique.

The SAXS curves of the synthesized PEEAs measured at room temperature are displayed in Fig. 6. All curves reveal a broad small-angle maximum in the region

Table 5 The d -spacings (in Å) calculated from SAXS and WAXS patterns of the PEAA samples

	PEAA4	PEAA6	PEAA8
First order	65	74	81
Fourth order	18.1	18.7	20.4
Sixth order	11.6	12.7	13.1
eighth order	8.6	9.1	–
Tenth order	6.4	–	–
120	4.26	4.34	4.40
060	3.85	3.87	3.88
140	–	3.71	–

**Fig. 7** WAXS curves of PEAA samples measured at room temperature

from 0.006 to 0.03 \AA^{-1} . This maximum can be attributed to the characteristic interference peak from the crystalline lamellar stack with the long period of 65, 74 and 81 \AA for PEAA4, PEAA6 and PEAA8, respectively. The increase in the long period is related to increase in the alkylene spacer length and therefore of the corresponding length of the crystallizable fragment. Two wide-angle reflections were identified as the fourth and sixth orders of the main SAXS peak (cf. Table 5), similarly to those found earlier by Lotz and co-authors for a poly(ester amide) [35].

An additional piece of information on the semicrystalline structure was extracted from the WAXS curves (cf. Fig. 7). In the range 0.07–0.18 \AA^{-1} , a series of broad maxima can be observed which were indexed as higher orders of the fundamental SAXS peak mentioned above (see Table 5). Interestingly, the peaks are better pronounced for the PEAA4 sample indicating sharper electron density contrast along the polymer chain. In contrast, for PEAA8 only the sixth order of the main

Table 6 Unit cell parameters calculated from the WAXS measurements

	PEAA4	PEAA6	PEAA8
$a, \text{\AA}$	4.59	4.72	4.75
$b, \text{\AA}$	23.26	23.31	23.30

peak was detected on the WAXS curve that may point on the presence of conformational defects in the main chain. The clear dependence of the long period on the alkyl spacer length of the PEAA's and observation of many orders of the main SAXS interference peak prompts suggesting that the crystals are built by the polymer chains in the extended-chain conformation. As far as the wide-angle peaks are concerned, i.e., the ones located in the range of $0.18\text{--}0.28 \text{\AA}^{-1}$, two relatively narrow peaks are observed for the PEAA6 and PEAA8 samples. According to previous works, the peaks are attributed to the inter-chain distances in the orthorhombic unit cell [35]. The peaks' indexation is presented in Table 5. The a and b parameters computed in the hypothesis of the orthorhombic unit cells are given in Table 6. It is noteworthy that the c parameter obviously cannot be estimated from the d -spacings of the only observed $hk0$ reflections. One can see that the lateral unit cell parameters are closed for all the polymers. A somewhat different a parameter for the PEAA4 sample can be explained by broadening of the WAXS peaks, which is probably caused by a smaller crystal size in the direction normal to the chain axis.

Conclusions

Poly(ester amide amide)s (PEAA's) of high molecular weight have been synthesized via a two-step melt polycondensation technique from preformed α,ω -aminoalcohols containing an amide group and dicarboxylic methyl esters of varying alkylene chain lengths. All the polymers exhibit a melt transition at around $135 \text{ }^\circ\text{C}$ and thermal degradation above $350 \text{ }^\circ\text{C}$. As shown from the DSC data, the crystallization rate decreases but the crystallinity increases with the increase in the alkylene chain length of the dicarboxylic acid methyl ester used in the polycondensation. Both DSC and TGA data testify that the synthesized PEAA's can be further melt processed without degradation as the decomposition temperatures of these PEAA's are significantly higher than their melting temperatures. X-ray scattering experiments in small and wide angles reveal formation of crystals with extended-chain conformation resulting in strict periodicity of electron density along the main chain. The chain packing in the direction normal to the chain axis is similar for all the studied PEAA's. One can speculate that the crystal structure is formed by regular hydrogen bonding network typical of polyamides. The obtained characteristics of the newly synthesized PEAA's can open new perspectives for fabrication of films, highly oriented fibers and injection-molded parts with good thermal stability and mechanical performance.

Acknowledgements The authors acknowledge the Ministry of Education and Science of the Russian Federation for financial support (contract No. 14.578.21.0190 (RFMEFI57816X0190)).

References

1. Kaplan DL, Thomas E, Ching C (1993) Biodegradable materials and packaging. Technomic Press, Lancaster
2. Moore GF, Saunders SM (1997) Advances in biodegradable polymers. Rapra review reports: 9/2. Rapra Technology Limited, Shropshire
3. Gonsalves KE, Chen X, Cameron JA (1992) Degradation of nonalternating poly(ester amides). *Macromolecules* 25:3309–3312
4. Wiegand S, Steffen M, Steger R, Koch RJ (1999) Isolation and identification of microorganisms able to grow on the polyester amide BAK. *J Environ Polym Degrad* 7:145–156
5. Lee S, Park JW, Yoo YT, Im SS (2002) Hydrolytic degradation behaviour and microstructural changes of poly(ester-co-amide)s. *Polym Degrad Stabil* 78:63–71
6. Qian ZY, Li S, He Y, Li C, Liu XB (2003) Synthesis and thermal degradation of biodegradable polyesteramide based on ϵ -caprolactone and 11-aminoundecanoic acid. *Polym Degrad Stabil* 81:279–286
7. Qian ZY, Sai L, He Y, Li C, Liu X (2003) Synthesis, characterization and in vitro degradation of biodegradable polyesteramide based on lactic acid. *Colloid Polym Sci* 281:869–875
8. Alla A, Rodriguez-Galan A, Martinez-de-Illarduya A, Munoz-Guerra S (1997) Degradable poly(ester amide)s based on l-tartaric acid. *Polymer* 38:4935–4944
9. Botines E, Rodriguez-Galan A, Puiggali J (2002) Poly(ester amide)s derived from 1,4-butanediol, adipic acid and 1,6-aminohexanoic acid: characterization and degradation studies. *Polymer* 43:6073–6084
10. Ferre T, Franco L, Rodriguez-Galan A, Puiggali J (2003) Poly(ester amide)s derived from 1,4-butanediol, adipic acid and 6-aminohexanoic acid. Part II: composition changes and fillers. *Polymer* 44:6139–6152
11. Armelin E, Paracuellos N, Rodriguez-Galan A, Puiggali J (2001) Study on the degradability of poly(ester amide)s derived from the α -amino acids glycine, and L-alanine containing a variable amide/ester ratio. *Polymer* 42:7923–7932
12. Kawasaki N, Nakayama A, Maeda Y, Hayashi K, Yamamoto N, Aiba S (1998) Synthesis of a new biodegradable copolyesteramide: poly(L-lactic acid-co- ϵ -caprolactam). *Macromol Chem Phys* 199:2445–2451
13. Perez-Rodriguez A, Alla A, Fernandez-Santin JM, Munoz-Guerra S (2000) Poly(ester amide)s derived from tartaric and succinic acids: changes in structure and properties upon hydrolytic degradation. *J Appl Polym Sci* 78:486–494
14. Andini S, Ferrara L, Maglio G, Palumbo R (1988) Synthesis of block polyesteramides containing biodegradable poly(L, L-lactide) segments. *Macromol Chem Rapid Commun* 9:119–124
15. Castaldo L, de Candia F, Maglio G, Palumbo R, Strazza G (1982) Synthesis and physico-mechanical properties of aliphatic polyesteramides. *J Appl Polym Sci* 27:1809
16. Castaldo L, Maglio G, Palumbo R (1992) Synthesis and preliminary characterization of polyesteramides containing enzymatically degradable amide bonds. *Polym Bull* 28:301–307
17. Pivsa-Art S, Nakayama A, Kawasaki N, Yamamoto N, Aiba S (2002) Biodegradability study of copolyesteramides based on diacid chlorides, diamines, and diols. *J Appl Polym Sci* 27:774–784
18. Bera S, Jedlinski Z (1992) Block/segmented polymer: 2. Studies on the thermal and mechanical properties of poly(amide ester)-ester copolymer. *Polymer* 33:4331–4336
19. Bera S, Jedlinski Z (1993) Block/segmented polymers. A new method of synthesis of copoly(amide-ester)-ester polymer. *J Polym Sci A Polym Chem* 31:731–739
20. Stapert HR, Dijkstra PJ, Feijen J (1998) Synthesis and characterization of aliphatic poly(esteramide)s containing symmetrical bisamide blocks. *Macromol Symp* 130:91–102
21. Dijkstra PJ, Stapert HR, Feijen J (2000) Synthesis of aliphatic poly(ester-amide)s containing uniform bisamide-bisester blocks. *Macromol Symp* 152:127–137
22. Lips PAM, Broos R, van Heeringen MJM, Dijkstra PJ, Feijen J (2005) Synthesis and characterization of poly(ester amide)s containing crystallizable amide segment. *Polymer* 46:7823–7833
23. Garg P, Keul H, Klee D, Möller M (2009) Thermal properties of poly(ester amide)s with isolated, two adjacent and three adjacent amide groups within a polyester chain. *Macromol Chem Phys* 20:1754–1765
24. Holden G, Legge NR, Quirk R, Schroeder MJM (1996) Thermoplastic elastomers. Hanser, New York

25. Odarchenko Y, Doblas D, Rosenthal M, Broos R, Hernandez J, Soloviev M, Anokhin DV, Vidal L, Feijen J, Sijbrandi N, Mes E, Kimenai A, Bar G, Dijkstra P, Ivanov DA (2014) Primary chemical sequence ultimately determines crystal thickness in segmented all-aliphatic co-polymers. *Macromolecules* 47(22):7890–7899
26. Odarchenko YI, Sijbrandi NJ, Rosenthal M, Kimenai AJ, Mes EPC, Broos R, Bar G, Dijkstra PJ, Feijen J, Ivanov DA (2013) Structure formation and hydrogen bonding in all-aliphatic segmented copolymers with uniform hard segments. *Acta Biomater* 9:6143–6149
27. Sijbrandi NJ, Kimenai AJ, Mes EPC, Broos R, Bar G, Rosenthal M, Odarchenko YI, Ivanov DA, Dijkstra PJ, Feijen J (2012) Synthesis, morphology and properties of segmented poly(ether ester amide)s comprising uniform glycine or β -alanine extended bisoxalamide hard segments. *Polymer* 53:4033–4044
28. Sijbrandi NJ, Kimenai AJ, Mes EPC, Broos R, Bar G, Rosenthal M, Odarchenko Y, Ivanov DA, Dijkstra PJ, Feijen J (2012) Synthesis, morphology and properties of segmented poly(ether amide)s with uniform oxalamide based hard segments. *Macromolecules* 45:3948–3961
29. Okada M (2002) Chemical syntheses of biodegradable polymers. *Prog Polym Sci* 27:87–133
30. Stapert HR, Bouwen AM, Dijkstra PJ, Feijen J (1999) Environmentally degradable aliphatic poly(ester-amide)s based on short, symmetrical and uniform bisamide-diol blocks. 1. Synthesis and interchange reactions. *Macromol Chem Phys* 200:1921–1929
31. Garg P, Keul H, Klee D, Möller M (2009) Concept and synthesis of poly(ester amide)s with one isolated, two or three consecutive amide bonds randomly distributed along the polyester backbone. *Des Monomers Polym* 12:405–424
32. Kohan MI (1995) *Nylon plastics handbook*. Hanser Publishers, Munich
33. Melnikov AP, Rosenthal M, Rodygin AI, Doblas D, Anokhin DV, Burghammer M, Ivanov DA (2016) Re-exploring the double-melting behavior of semirigid-chain polymers with an in situ combination of synchrotron nano-focus X-ray scattering and nanocalorimetry. *Eur Polym J* 81:598–606
34. Ivanov DA, Jonas AM, Legras R (2000) The crystallization of poly(aryl-ether-ether-ketone) (PEEK). Reorganization processes during gradual reheating of cold-crystallized samples. *Polymer* 41:3719–3727
35. Paredes N, Casas MT, Puiggali J, Lotz B (1999) Structural data on the packing of poly(ester amide)s derived from glycine, hexanediol, and odd-numbered dicarboxylic acids. *J Polym Sci B Polym Phys* 37:2521–2533